Structural Analysis of Human Serum Albumin Complexes with Cationic Lipids

David Charbonneau, Marc Beauregard, and Heidar-Ali Tajmir-Riahi*

Département de Chimie-Biologie, Université du Québec à Trois-Rivières, C. P. 500, Trois-Rivières (Québec), G9A 5H7, Canada

Received: October 17, 2008

Human serum albumin (HSA) is a major transporter for delivering several endogenous compounds including fatty acids *in vivo*. Even though HSA is the primary target of fatty acid binding, the effects of cationic lipid on protein stability and conformation have not been investigated. The aim of this study was to examine the interaction of human serum albumin (HSA) with helper lipids—cholesterol (Chol) and dioleoylphosphatidylethanolamine (DOPE)—and with cationic lipids—dioctadecyldimethylammonium bromide (DDAB) and 1,2-dioleoyl-3-trimethylammonium-propane (DOTAP), at physiological conditions, using constant protein concentration and various lipid contents. Fourier transform infrared (FTIR), circular dichroism (CD), and fluorescence spectroscopic methods were used to analyze the lipid binding mode, the binding constant, and the effects of lipid interaction on HSA stability and conformation. Structural analysis showed that cholesterol and DOPE (helper lipids) interact mainly with HSA polypeptide polar groups and via hydrophobic moieties. Hydrophobic interactions dominate the binding of cationic lipids to HSA. The number of bound lipids (n) calculated was 1.22 (cholesterol), 1.82 (DDAB), 1.76 (DOPE), and 1.56 (DOTAP). The overall binding constants estimated were $K_{Chol} = 2.3\ (\pm 0.50) \times 10^3\ M^{-1}$, $K_{DDAB} = 8.9\ (\pm 0.95) \times 10^3\ M^{-1}$, $K_{DOTAP} = 9.1\ (\pm 0.90) \times 10^3\ M^{-1}$, and $K_{DOPE} = 4.7\ (\pm 0.70) \times 10^3\ M^{-1}$. HSA conformation was stabilized by cholesterol and DOPE with a slight increase of protein α-helical structures, while DOTAP and DDAB induced an important ($\alpha \rightarrow \beta$) transition, suggesting a partial protein unfolding.

Introduction

Complexes of cationic lipids (Scheme 1) with DNA are used to deliver genetic information into cells for gene therapy and vaccines.[1] The inclusion of dioleoylphosphatidylethanolamine (DOPE) and cholesterol in cationic lipid preparations enhances DNA transfection. Human serum albumin (HSA, Scheme 2) is the most abundant serum protein, which carries several endogenous compounds including fatty acids.[2] HSA is the primary transporter for delivering fatty acids to tissues and contains at least seven specific fatty acids binding.[3] HSA has long been the center of attention of the pharmaceutical industry due to its ability to bind various drug molecules and alter their pharmacokinetic properties.[4] HSA is a globular protein composed of three structurally similar domains (I, II, and III), each containing two subdomains (A and B) and stabilized by 17 disulfide bridges.[5−12] Aromatic and heterocyclic ligands were found to bind within two hydrophobic pockets in subdomains IIA and IIIA, namely, site I and site II.[5−12] Seven binding sites for fatty acids are localized in subdomains IB, IIIA, and IIIB and on the subdomain interfaces.[5] HSA has also a high affinity metal-binding site at the N-terminus.[6] These multiple binding sites underline the exceptional ability of HSA to interact with many organic and inorganic molecules and make this protein an important regulator of intercellular fluxes, as well as the pharmacokinetic behavior of many drugs.[5−13] Even though the binding sites of fatty acids on HSA have been located, the interaction of cationic lipids with HSA has not been fully investigated. Therefore, it was of interest to study the binding of cationic lipids with HSA in aqueous solution, in order to examine the effects of lipid complexation on protein secondary structure, conformation, and stability. In this Article, we present a spectroscopic analysis of the interaction of HSA with the cationic lipids dioctadecyldimethylammonium bromide (DDAB) and 1,2-dioleoyl-3-trimethylammonium-propane (DOTAP) and with the helper lipids cholesterol and DOPE (Scheme 1) in aqueous solution at physiological conditions, using constant protein concentration and various lipid contents. Structural information regarding lipid binding mode and the effects of lipid−HSA complexation on the protein stability and secondary structure is reported here.

Experimental Section

Materials. HSA fraction V was purchased from Sigma Chemical Company and used as supplied. Cholesterol (Chol), DOTAP, DDAB, and DOPE were from Avanti Polar Lipid Inc., and used as supplied. Other chemicals were of reagent grade and used without further purification. Human serum albumin was dissolved in aqueous solution (40 mg/mL or 0.5 mM) in 10 mM Tris−HCl buffer (pH 7.4). The protein concentration was determined by absorption measurements using an extinction coefficient of 36 500 $M^{-1}\ cm^{-1}$ at 280 nm.[14] In this study, HSA did not have its fatty acids removed, in a way to reproduce normal physiological conditions, where between 0.1 and 2 fatty acid molecules are bound to albumin.[6,12] A 2 mM lipid solution was first prepared in Tris−HCl/ethanol 50% and then diluted to 1, 0.5, and 0.25 mM in Tris−HCl/ethanol 50%. After addition of an equal volume of lipid solution to protein solution, the final ethanol concentration was reduced to 25%. The blank contains HSA in ethanol 25% as the baseline. The presence of ethanol 25% induces no major HSA structural changes according to a recent publication.[15]

Fourier Transform Infrared (FTIR) Measurements. Infrared spectra were recorded on a FTIR spectrometer (Impact

* Corresponding author. Fax: 819-376-5084. Phone: 819-376-5011(ext. 3310). E-mail: tajmirri@uqtr.ca.

10.1021/jp8092012 CCC: $40.75
Published on Web 01/14/2009

SCHEME 1: Structures of Lipids

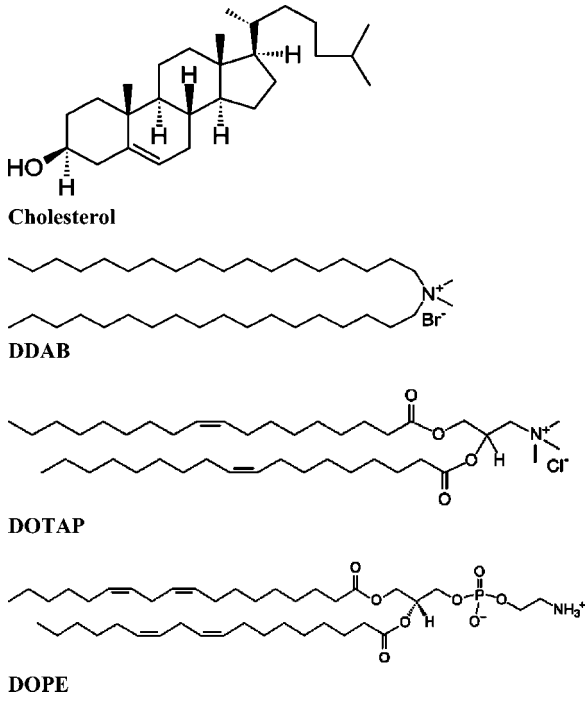

SCHEME 2: Chemical Structure of Human Serum Albumin

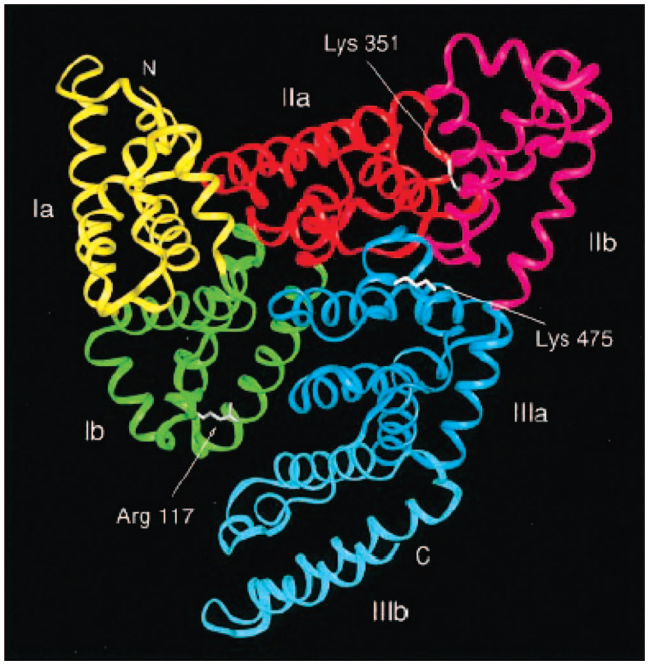

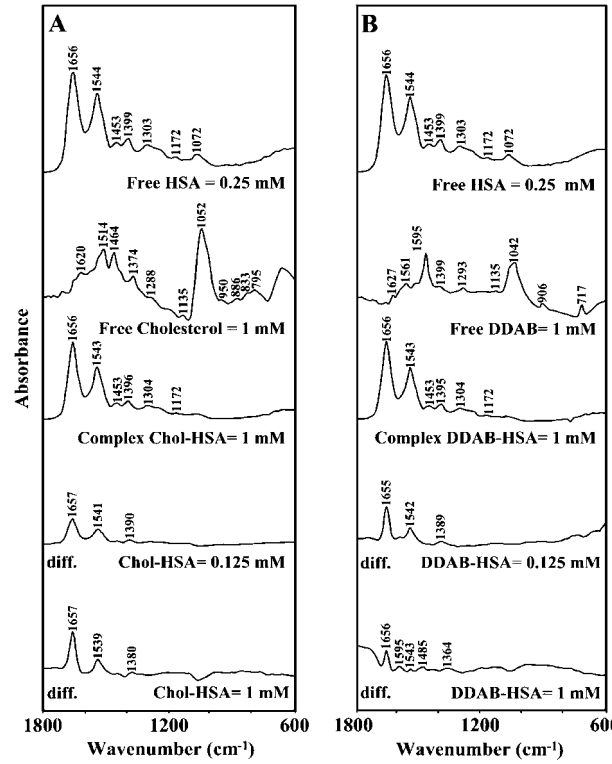

Figure 1. FTIR spectra in the region 1800−600 cm^{-1} of hydrated films (pH 7.4) for free HSA (0.25 mM), free Chol (1 mM), and Chol−HSA (A), free DDAB (1 mM) and DDAB−HSA (B) (top three curves) and difference spectra (diff.) of lipid−HSA complexes (bottom two curves) obtained at different lipid concentrations (indicated on the figure).

420 model), equipped with a deuterated triglycine sulfate (DTGS) detector and KBr beam splitter, using AgBr windows. A solution of lipid was added dropwise to the protein solution with constant stirring to ensure the formation of homogeneous solution and to reach the target lipid concentrations of 0.125, 0.25, 0.5, and 1 mM with a final protein concentration of 0.25 mM (20 mg/mL). Spectra were collected after 2 h of incubation of HSA with lipid solution at room temperature as hydrated films. Interferograms were accumulated over the spectral range 4000−600 cm^{-1} with a nominal resolution of 4 cm^{-1} and 100 scans. The difference spectra [(protein solution + lipid solution) − (protein solution)] were generated using the polypeptide antisymmetric and symmetric C−H stretching bands,[16] located at 2900−2800 cm^{-1}, as an internal standard. These bands, which are due to protein C−H stretching vibrations, do not undergo any spectral changes (shifting or intensity variation) upon lipid complexation, and therefore, they are commonly used as an internal standard. When producing difference spectra, these bands were adjusted to the baseline level, in order to normalize the difference spectra. Details regarding infrared spectral treatment are given in our recent publication.[17]

Analysis of the secondary structure of HSA and its lipid complexes was carried out on the basis of the procedure already reported.[18] The protein secondary structure is determined from the shape of the amide I band, located at 1660−1650 cm^{-1}. Fourier self-deconvolution and second derivative resolution enhancement were applied to increase the spectral resolution in the region 1700−1600 cm^{-1} and fitted the position of the bands. In order to quantify the area of the different components of the amide I contour, revealed by self-deconvolution and the second derivative, a least-squares iterative curve fitting was used to fit the Gaussian line shapes to the spectra between 1700 and 1600 cm^{-1}. The details of spectral manipulation regarding curve fitting have been previously reported.[19] The curve-fitting analysis was performed using the GRAMS/AI Version 7.01 software of the Galactic Industries Corporation.

Circular Dichroism (CD). CD spectra of HSA and its lipid complexes were recorded with a Jasco J-720 spectropolarimeter. For measurements in the far-UV region (178−260 nm), a quartz cell with a path length of 0.01 cm was used in a nitrogen atmosphere. The HSA concentration was kept constant (12.5 μM) while varying each lipid concentration (0.25, 0.5, and 1 mM). An accumulation of five scans with a scan speed of 50 nm/min was performed, and data were collected for each nanometer from 260 to 180 nm. The sample temperature was

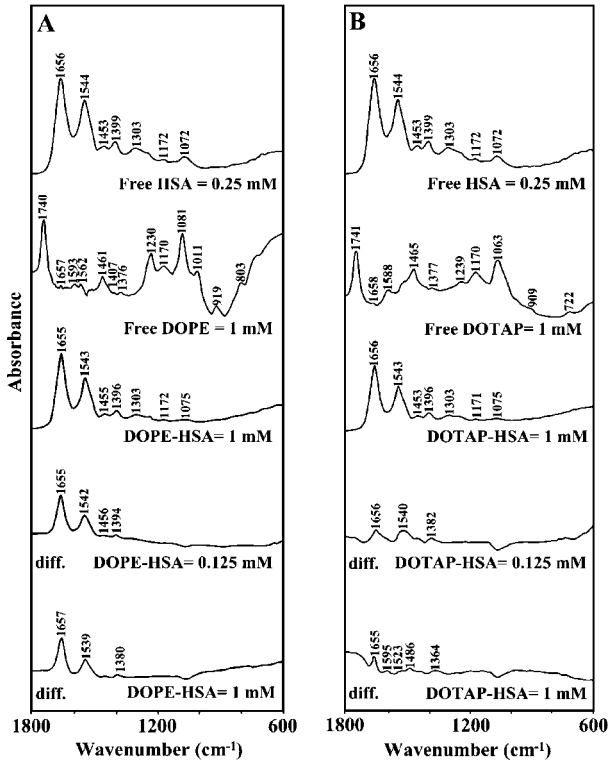

Figure 2. FTIR spectra in the region 1800−600 cm^{-1} of hydrated films (pH 7.4) for free HSA (0.25 mM), free DOPE (1 mM), and DOPE−HSA (A), free DOTAP (1 mM) and DOTAP−HSA (B) (top three curves) and difference spectra (diff.) of lipid−HSA complexes (bottom two curves) obtained at different lipid concentrations (indicated on the figure).

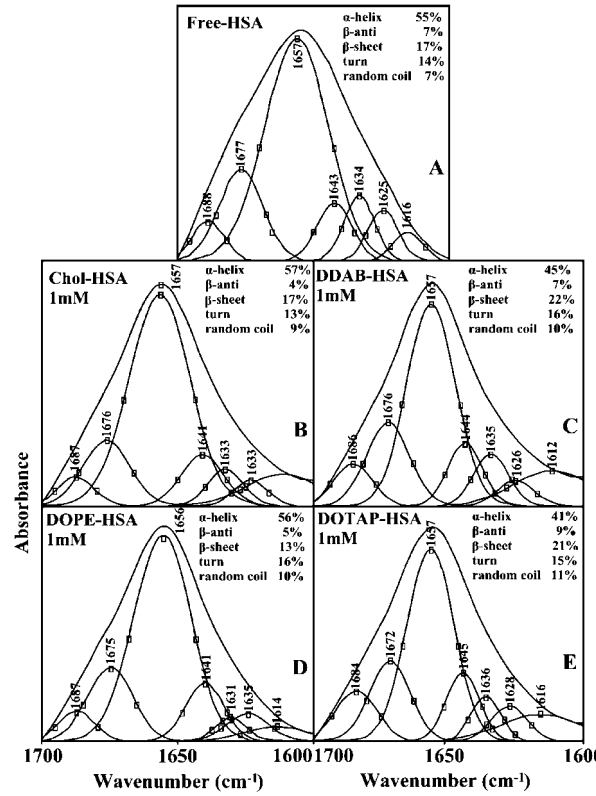

Figure 3. Second derivative resolution enhancement and curve-fitted amide I region (1700−1600 cm^{-1}) for free HSA and its lipid adducts in aqueous solution with 1 mM lipid and 0.25 mM protein concentrations at pH 7.4.

maintained at 25 °C using a Neslab RTE-111 circulating water bath connected to the water-jacketed quartz cuvettes. Spectra were corrected for buffer signal, and conversion to the Mol CD ($\Delta\varepsilon$) was performed with the Jasco Standard Analysis software. The protein secondary structure was calculated using CDSSTR, which calculates the different assignments of secondary structures by comparison with CD spectra, measured from different proteins for which high quality X-ray diffraction data are available.[20,21] The program CDSSTR is provided in the CDPro software package which is available at the Web site http://lamar.colostate.edu/~sreeram/CDPro.

Absorption Spectra. The absorption spectra were recorded on a Perkin-Elmer Lambda 40 Spectrophotometer. Quartz cuvettes of 1 cm were used for determination of protein concentration.

Fluorescence Spectroscopy. Fluorometric experiments were carried out on a Varian Cary Eclipse. Various solutions of lipid (10−400 μM) Tris−HCl/ethanol 50% were prepared from the above stock solutions by successive dilutions. A solution of HSA (10 μM) in 10 mM Tris−HCl (pH. 7.4) was prepared. The above solutions were kept in the dark and used soon after preparation. Equal volumes of the above HSA solution and of the various lipid solutions were mixed to obtain a final lipid concentration of 5−200 μM with a constant HSA content of 5 μM (in 25% ethanol). The fluorescence spectra were recorded with an excitation wavelength of λ_{exc} = 280 nm, and fluorescence emission spectra were recorded from λ_{em} = 287 nm to λ_{em} = 500 nm. The intensity at 330 nm (tryptophan) was used to calculate the binding constant (K) according to previous literature reports.[22−25]

Results and Discussion

FTIR Spectra of Lipid−HSA Complexes. Strong lipid−HSA complexation was suggested by infrared spectroscopic results, since there was no major spectral shifting for the protein amide I band at 1656 cm^{-1} (mainly C═O stretch) and amide II band at 1544 cm^{-1} (C−N stretching coupled with N−H bending modes),[16−18] upon lipid interaction. The difference spectra [(protein solution + lipid solution) − (protein solution)] were obtained, in order to monitor the intensity variations of these vibrations, and the results are shown in Figures 1 and 2. Similarly, the infrared self-deconvolution with second derivative resolution enhancement and curve-fitting procedures[18] were used to determine the protein secondary structure in the presence of lipid (Figure 3 and Table 1). At low lipid concentration (125 μM), intensity changes were observed for the protein amide I at 1656 and amide II bands at 1544 cm^{-1}, in the difference spectra of lipid−HSA complexes (Figures 1 and 2, diff. 0.125 mM). Positive features are located for amide I and II bands at 1657, 1541 cm^{-1} for Chol−HSA and at 1655, 1542 cm^{-1} for DOPE−HSA complexes. Difference positive features were also observed at 1655, 1542 and 1656, 1540 cm^{-1} for DDAB−HSA and DOTAP−HSA, respectively. These positive features are related to an increase in the intensity of the amide I and amide II bands upon lipid complexation (Figures 1 and 2, diff. 0.125 mM). The increase in intensity of the amide I and amide II bands, mainly C═O and C−N vibrations, indicate structural changes in intramolecular bonding and may come from the impact of lipid interaction on the overall protein conformation. Additional evidence to support the effect of lipid interactions on HSA comes from the shifting of the protein amide A band at 3296 cm^{-1} (N−H stretching mode) in the free HSA to 3298 cm^{-1} (Chol−HSA), 3293 cm^{-1} (DOPE−HSA), 3294 cm^{-1}

TABLE 1: Secondary Structure Analysis (Infrared Spectra) for the Free HSA and Its Lipid Complexes in Hydrated Film at pH 7.4

amide I components (cm^{-1})	free HSA (%) 0.25 mM	Chol−HSA (%) 1 mM	DOPE−HSA (%) 1 mM	DDAB−HSA (%) 1 mM	DOTAP−HSA (%) 1 mM
1692−1680 β-anti	7 ± 1	4 ± 1	5 ± 1	7 ± 1	9 ± 1
1680−1660 turn	14 ± 1	13 ± 2	16 ± 2	16 ± 2	15 ± 2
1660−1650 α-helix	55 ± 2	57 ± 1	56 ± 2	45 ± 2	41 ± 2
1648−1641 random coil	7 ± 1	9 ± 1	10 ± 1	10 ± 1	11 ± 1
1640−1610 β-sheet	17 ± 1	17 ± 1	13 ± 1	22 ± 2	21 ± 2

(DDAB−HSA), and 3294 cm^{-1} (DOTAP−HSA) upon lipid complexation.

As the lipid concentration was increased to 1 mM, strong positive features in the amide I and II bands were observed at 1657 and 1539 cm^{-1} for both the Chol−HSA and DOPE−HSA complexes, while reduction of the amide I and II bands at 1656, 1543 cm^{-1} and at 1655, 1523 cm^{-1} occurred for DDAB−HSA and DOTAP−HSA compared to low lipid concentration in the difference spectra of lipid−protein complexes (Figures 1 and 2, diff, 1 mM). The observed increase in intensity of the amide I and II bands in the spectra of Chol−HSA and DOPE−HSA suggests minor alteration, involving a change in intramolecular hydrogen bonding, while the decrease in the intensity of the amide I and II bands for DDAB−HSA and DOTAP−HSA complexes compared to low lipid concentration suggests major protein conformational changes upon lipid−protein interaction possibly caused by a reorganization of intra- and intermolecular hydrogen bonding. Similar infrared spectral changes have been observed for the protein amide I band in several drug−HSA complexes, where major protein conformational changes occurred.[26] Precipitation of HSA led to increased turbidity when the protein was treated with 1 mM DDAB and DOTAP (Figures 1 and 2, diff., 1 mM).

A quantitative analysis of the protein secondary structure for the free HSA and its lipid adducts in hydrated films has been carried out, and the results are shown in Figure 3 and Table 1. The free protein has 55% α-helix (1657 cm^{-1}), 17% β-sheet (1616, 1625, and 1634 cm^{-1}), 14% turn structure (1677 cm^{-1}), 7% β-antiparallel (1688 cm^{-1}), and 7% random coil (1643 cm^{-1}) (Figure 4A and Table 1). The β-sheet structure is composed of three components at 1616 (intermolecular β-sheet), 1625 (intramolecular β-sheet), and 1634 cm^{-1} (hydrated) that are consistent with the spectroscopic studies of human serum albumin.[27−29] Upon lipid interaction, a minor increase of the α-helix from 55% (free HSA) to 57% (Chol−HSA) and 56% (DOPE−HSA) with a decrease of the β-sheet from 17% (free HSA) to 13% (DOPE−HSA) were observed (Figure 3 and Table 1). These results are consistent with the increase in the intensity of the protein C═O stretching band mentioned above. However, a major decrease of the α-helix from 55% (free HSA) to 45% (DDAB−HSA) and 41% (DOTAP−HSA) with an increase of β-sheet structure from 17% (free HSA) to 22% (DDAB−HSA) and 21% (DOTAP−HSA) were observed (Table 1). The structural analysis suggests important differences in the binding modes of Chol and DOPE compared to DDAB and DOTAP−protein complexes. The binding of Chol and DOPE leads to a slight increase in α-helix content. The nature of the Chol−HSA and DOPE−HSA interaction seems to be very similar. Stabilizing hydrogen bonding seems to be the major binding mode in the Chol−protein and DOPE−protein complexes. The effect of H bonding between the HSA polar group and the cholesterol hydroxyl group and between HSA (N−H groups) and DOPE carbonyl groups was very similar and induced protein stabilization, while DDAB and DOTAP complexation suggest a partial protein unfolding leading to precipitation at high lipid concentration.

Hydrophobic Interactions. The impact of complexation on lipid antisymmetric and symmetric CH_2 stretching vibration in the region 3000−2800 cm^{-1} was investigated by infrared spectroscopy. Free cholesterol CH_2 bands at 2956, 2935, and 2866 cm^{-1} shifted to 2958, 2935, and 2871 cm^{-1} after complexation (Chol−HSA); free DDAB CH_2 bands at 2951, 2917, and 2847 cm^{-1} shifted to 2957, 2919, and 2850 cm^{-1} (DDAB−HSA); free DOPE at 2953, 2925, and 2854 cm^{-1} shifted to 2958, 2936, and 2871 cm^{-1} (DOPE−HSA); and free DOTAP at 2956, 2925, and 2854 cm^{-1} shifted to 2957, 2935, and 2871 cm^{-1} (DOTAP−HSA), in the lipid−protein complexes (Figure 4). Major shifting of the lipid antisymmetric and symmetric CH_2 stretching vibrations in the region 3000−2800 cm^{-1} of the infrared spectra suggests the presence of hydrophobic interactions *via* lipid aliphatic tails and the hydrophobic region in HSA. The observed spectral shifting for the lipid CH_2 stretching modes is consistent with a major hydrophobic lipid−protein interaction *via* lipid aliphatic tails.

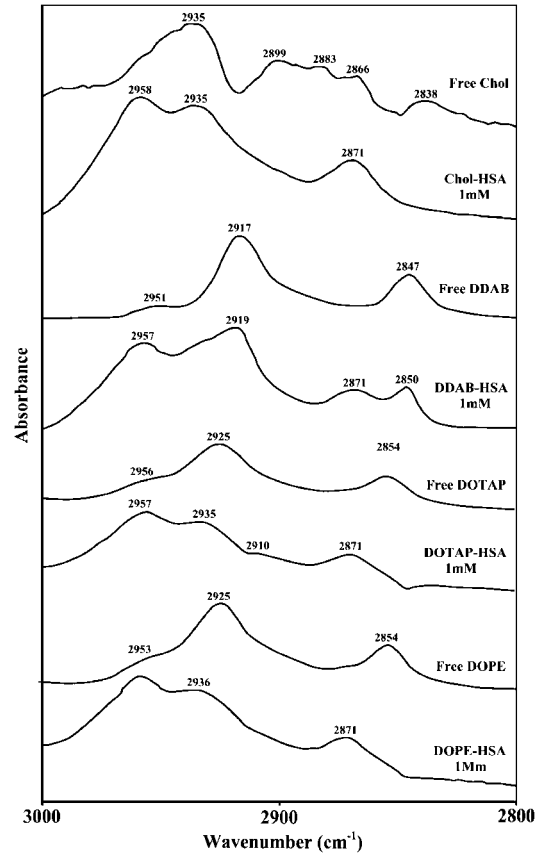

Figure 4. Spectral changes of lipid CH_2 symmetric and antisymmetric stretching vibrations upon HSA complexation (the contribution from free protein vibrations has been subtracted in this region).

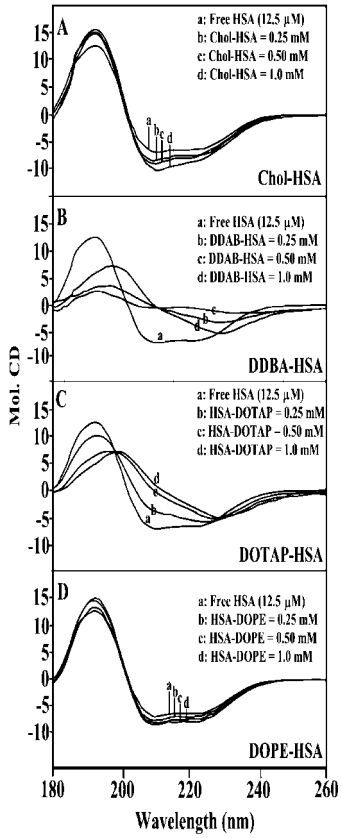

Figure 5. Circular dichroism of free HSA and its lipid complexes in aqueous solution with a protein concentration of 12.5 μM and lipid concentrations of 0.25, 0.5, and 1 mM in 5 mM Tris−HCl buffer pH 7.4, ethanol 25% (v/v) at 25 °C.

TABLE 2: Secondary Structure of HSA Complexes (CD Spectra) with Lipids at pH 7.4 (Calculated by CDSSTR Software)

lipid concentration (mM)	α-helix (±3%)	β-sheet (±2%)	turn (±2%)	random (±2%)
free HSA	59	14	14	13
Chol−HSA (1 mM)	62	19	10	9
DOPE−HSA (1 mM)	61	18	11	10
DOTAP−HSA (1 mM)	40	27	16	17
DDAB−HSA (1 mM)	41	30	15	14

CD Spectra. The CD spectroscopic results shown in Figure 5 and Table 2 exhibit marked similarities with those of the infrared data. Secondary structures calculated on the basis of CD data suggest that free HSA has a high α-helix content (59%), 15% in β-sheet, 14% in turn, and 13% in random region (Figure 5 and Table 2), which is consistent with the literature report.[30] A minor increase in the α-helix from 59% free protein to 62% for Chol−HSA and 61% for DOPE−HSA complexes occurred (Figure 5 and Table 2). The increase in α-helix was accompanied by an increase in β-sheet and turn structure, while a reduction in random coil structure was observed (Table 2). However, a major reduction of the α-helix from 59% (free HSA) to 41% (DDAB−HSA) and 40% (DOTAP−HSA) was observed, concomitant with a major increase in β-sheet from 14 to 30% and 27% for DDAB−HSA and DOTAP−HSA complexes, respectively. Similarly, turn and random structures were also increased (Figure 5 and Table 2). The CD data related to conformational changes of lipid−HSA are consistent with the infrared results that showed an increase of the α-helix for Chol−HSA and DOPE−HSA adducts and a major reduction of the α-helix for DDAB−HSA and DOTAP−HSA complexes, leading to conversion in β-sheet structure (Tables 1 and 2). These considerable conversions of α-helix to β-sheet structures can be correlated with precipitation due to denaturation by formation of agglomerated proteins. This can occur *via* intermolecular β-sheet formation, which may in turn lead to interprotein sheet structure.[31] The conformational changes observed *via* CD and IR results are indicative of a partial protein unfolding in the DDAB−HSA and DOTAP−HSA complexes, while similar interaction modes were suggested for Chol−HSA and DOPE−HSA complexes, inducing some degree of stabilization. It should be noted that a major reduction of intensity signal observed in CD spectra of 0.5 mM DDAB−HSA might be due to precipitation of the lipid−protein complex as the turbidity of solution was observed in the cuvette (Figure 5, 0.5 mM DDAB). There are some minor differences between IR and CD results regarding free HSA conformation (Tables 1 and 2). The reason for the differences may be due to sample preparation, since IR measurements were performed in hydrated films, whereas CD experiments were conducted in aqueous solutions. Similarly, lipid-to-HSA ratios were different in the two cases. Similar differences were also observed for several proteins where sample preparations were different for IR and CD measurements.[32]

Fluorescence Spectra. HSA contains a single polypeptide of 585 amino acids with only one tryptophan (Trp 214) located in subdomain IIA. Tryptophan 214 emission dominates HSA fluorescence spectra in the UV region. When other molecules interact with HSA, tryptophan fluorescence may change depending on the impact of such an interaction on the protein conformation, or *via* a direct quenching effect.[33] On the assumption that there are *n* substantive binding sites for quencher (Q) on protein (B), the quenching reaction can be shown as follows:

$$n\mathrm{Q} + \mathrm{B} \leftrightarrow \mathrm{Q}n\mathrm{B} \tag{1}$$

The binding constant (K_A) can be calculated as

$$K_A = [\mathrm{Q}_n\mathrm{B}]/[\mathrm{Q}^n][\mathrm{B}] \tag{2}$$

where [Q] and [B] are the quencher and protein concentration, respectively, and [Q_nB] is the concentration of the nonfluorescent fluorophore−quencher complex where [B_0] gives total protein concentration

$$[\mathrm{Q}_n\mathrm{B}] = [\mathrm{B}_0] - [\mathrm{B}] \tag{3}$$

$$K_A = [\mathrm{B}_0] - [\mathrm{B}]/[\mathrm{Q}^n][\mathrm{B}] \tag{4}$$

The fluorescence intensity is proportional to the protein concentration as described below:

$$[\mathrm{B}]/[\mathrm{B}_0] \propto F/F_0 \tag{5}$$

Results from fluorescence measurements can be used to estimate the binding constant of the lipid−protein complex. From eq 4,

$$\log[(F_0 - F)/F] = \log K_A + n \log[\mathrm{Q}] \tag{6}$$

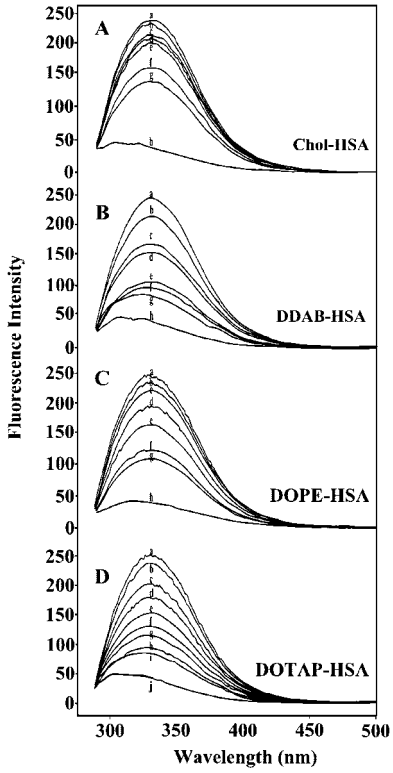

Figure 6. Fluorescence emission spectra of lipid−HSA systems in 10 mM Tris−HCl buffer pH 7.4, ethanol 25% (v/v) at 25 °C for (A) Chol−HSA [(a) free HSA; (b−g) 5 μM HSA with Chol at 10, 15, 20, 25, 50, and 100 μM; (h) 200 μM free cholesterol], (B) DDAB−HSA [(a) free HSA (5 μM); (b−g) 5 μM HSA with DDAB at 20, 25, 30, 35, 45, and 100 μM; (h) 200 μM free DDAB], (C) DOPE−HSA [(a) free HSA (5 μM); (b−g) 5 μM HSA with DOPE at 5, 10, 15, 25, 35, and 200 μM; (h) 200 μM free DOPE], and (D) DOTAP−HSA [(a) free HSA (5 μM); (b−i) 5 μM HSA with DOTAP at 5, 10, 15, 20, 25, 30, 35, and 50 μM; (j) 200 μM free DOTAP].

where F_0 is the initial fluorescence intensity and F is the fluorescence intensity in the presence of quenching agent. K_A is the quenching constant, and [Q] is the molar concentration of the quencher. The plot of log[$(F_0 - F)/F$] vs log[lipid] yields log K_A as the intercept on the y axis and n as the slope.[36,42] Thus, the antilog of the intercept gives K_A. The decrease of the fluorescence intensity of HSA has been monitored at 330 nm for HSA−lipid systems (Figure 6 shows representative results for each system). The plot of log[$(F_0 - F)/F$] vs log[lipid] (Figure 7 shows representative plots). The K values given here are averages of four-replicate and six-replicate runs for HSA−lipid systems, each run involving several different concentrations of lipid (Figure 7). The binding constants obtained were $K_{chol} = 2.3 \times 10^3$ M^{-1}, $K_{DDAB} = 8.9 \times 10^3$ M^{-1}, $K_{DOPTAP} = 9.1 \times 10^3$ M^{-1}, and $K_{DOPE} = 4.7 \times 10^3$ M^{-1} (Figure 7). The association constants calculated for the lipid−HSA suggest low affinity lipid−HSA binding, compared to the other strong ligand−protein complexes with binding constants ranging from 10^6 to 10^8 M^{-1}. However, lower binding constants (10^4−10^5 M^{-1}) were recently reported for several other ligand−protein complexes[4,34] using the fluorescence spectroscopic method[22,25,34–36] consistent with our results.

As a result, we predict that the only fluorophore Trp 214 is relatively buried inside the HSA. This argument is based on the fact that the emission λ_{max} of Trp 214 was 330 nm (Figure 6), which is the emission region of considerably hidden tryptophan molecules known to be usually around 320−325 nm,[37,38] while fluorescence emission of the exposed tryptophan

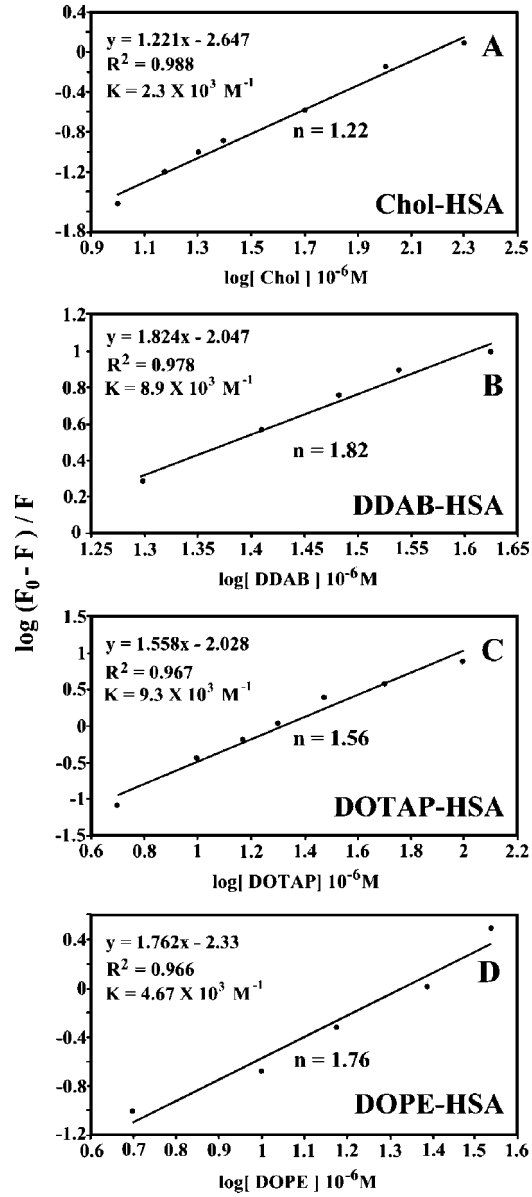

Figure 7. Plot of log[$(F_0 - F)/F$] as a function of log[lipid], the binding constant K being the ratio of the intercept and the slope for (A) Chol−HSA, (B) DDAB−HSA, (C) DOTAP−HSA, and (D) DOPE−HSA complexes with the number of bound lipids (n).

molecule is around 340 nm due to solvent relaxation. The HSA conformation seems to bury Trp 214 in a hydrophobic environment. The change in fluorescence intensity of Trp 214 in the presence of lipid may arise as a direct quenching effect or as a result of conformational changes induced after lipid binding to HSA. The results indicate that lipid interaction does not change the emission λ_{max} at 330 nm. No spectral shift was observed for the emission spectra upon lipid−HSA complexation, indicating that Trp 214 was not exposed to any change in polarity. The emission λ_{max} of quenched tryptophan remains at 330 nm, and the quenching may arise from lipid interaction on the overall HSA conformation or *via* the hydrophobic region located inside the protein, without disturbing the hydrophobic environment of Trp 214. Hydrophobic interactions are more probable, and this argument is consistent with the infrared analysis of lipid CH_2 antisymmetric and symmetric stretching vibration discussed earlier. These results suggest that cationic lipids can interact with HSA *via* the hydrophobic region by aliphatic tails. The number of ligands bound (n) can be calculated from log[(F_0 −

$F)/F] = \log K_S + n \log[\text{lipid}]$.[38−42] The linear plot of $\log[(F_0 - F]/F]$ as a function of log[lipid] is shown in Figure 7. The n values from the slope of the straight line are 1.22 (cholesterol), 1.82 (DDAB), 1.56 (DOTAP), and 1.76 (DOPE) (Figure 7). The larger bindings observed for DDAB ($n = 1.82$) are consistent with major perturbations of HSA secondary structure inducing protein unfolding.

The results obtained from these different spectroscopic methods consistently show that major perturbations of protein secondary structure occurred for cationic lipids, DDAB−HSA and DOTAP−HSA complexes, and that they are involved in different binding modes from those of the Chol−HSA and DOPE−HSA complexes. FTIR and CD data show that cationic lipids, DDAB and DOTAP, induce a partial protein unfolding, while Chol and DOPE complexes lead to a slight increase in protein α-helical structures. Both hydrophilic and hydrophobic interactions occur for Chol and DOPE−HSA adducts. FTIR data show that neutral cholesterol and zwiterionic DOPE interact with polypeptide polar groups. Cholesterol hydroxyl groups and DOPE carbonyl groups (C═O) can form hydrogen bonds with polypeptide polar groups in the surface of HSA. Some hydrophobic interactions via hydrophobic moieties were also suggest by the FTIR data, but hydrophilic interactions dominate the binding of Chol and DOPE to HSA. Data suggest that hydrophobic interaction via aliphatic tails dominates the binding of cationic lipids to HSA. The electrostatic effect between cationic head groups and the positive amino acid side chain, e.g., lysine, arginine, and histidine, may explain the minor binding of cationic lipids *via* polar heads; therefore, hydrophobic interaction should dominate the complexation of cationic lipids with HSA. These can explain the major differences between DOPE−HSA and DOTAP−HSA complexes for which similar carbonyl groups are present at the lipid polar head. The electrostatic effects repulse the DOTAP cationic and DDAB head groups and force these cationic lipids to interact by the hydrophobic effect. Consistent with the infrared analysis of lipid CH_2 antisymmetric and symmetric stretching vibration, these results suggest that cationic lipids can interact with the HSA hydrophobic region *via* aliphatic tails. The part of hydrophobic amino acids that forms hydrophobic cavities in each domain may interact with the aliphatic tails of cationic lipids consistent with different hydrophobic pockets that accommodate the alkyl chain of fatty acids (39). Referring to the crystallographic analysis of HSA fatty acid binding sites (2), three potential binding sites of cationic lipids are identified regarding the Trp 214 quenching: sites 8, containing Trp 214, and close to the sites 7 and 6. Fluorescence results show that the interaction of lipids does not change the hydrophobic environment of the fluorophore. The interaction of lipids seems to remain in the subdomain where Trp 214 is located (i.e., IIA), in the hydrophobic environment. The binding constant of lipid−HSA complexes calculated from fluorescence data shows moderate lipid−HSA interaction. The present interpretation is supported by the binding constants obtained for different lipid−HSA complexes. The electrostatic effects between cationic head groups and the positive amino acid side chain may affect the quenching of cationic lipids and explain the low value of binding constants. Neutral molecules, cholesterol, and zwitterionic DOPE bind weaker than cationic lipids. This result can be explained by the nature and the site of interaction for which less quenching effect results. The larger bindings observed for DDAB ($n = 1.82$) are consistent with major perturbations of HSA secondary structure inducing protein unfolding. Even though DOPE seems to bind HSA with a relatively large number (n), its sites of interaction must be different from DDAB and DOTAP in which lipid complexation causes more impact on HSA conformation than DOPE and cholesterol.

Conclusions

In conclusion, on the basis of our spectroscopic data on lipid−HSA complexes, different binding patterns were observed for DDAB and DOTAP compared with cholesterol and DOPE. The binding of DDAB and DOTAP leads to important HSA conformational changes characterized by an $\alpha \rightarrow \beta$ transition, suggesting a partial protein unfolding, leading to precipitation at high lipid concentration (1 mM), whereas cholesterol and DOPE interactions induce a small increase in α-helical content, indicating protein structural stabilization. Both hydrophilic and hydrophobic interactions occur for lipid−protein complexes.

Acknowledgment. This work is supported by a grant from Natural Sciences and Engineering Research Council of Canada (NSERC). D.C. acknowledges the CREFSIP, Université LAVAL.

Note Added after ASAP Publication. This article posted ASAP on January 14, 2009 with an error in equation 3. The final correct version posted January 16, 2009.

References and Notes

(1) Templeton, N. S. *Gene Therapy:Therapeutic mechanisms and strategies*, 2nd ed.; Dekker: New York, 2004.
(2) Simard, J. R.; Zunszain, P. A.; Ha, C. E.; Yanhg, J. S.; Bhagavan, N. V.; Petipas, I.; Curry, S.; Hamilton, J. A. *Proc. Natl. Acad. Sci. U.S.A.* **2005**, *102*, 17958.
(3) Bhattacharya, A. A.; Grune, T.; Curry, S. *J. Mol. Biol.* **2000**, *303*, 721.
(4) Kratochwil, N. A.; Huber, W.; Muller, F.; Kansy, M.; Gerber, P. R. *Biochem. Pharmacol.* **2002**, *64*, 1355.
(5) Sugio, S.; Kashima, A.; Mochizuki, S.; Noda, M.; Kobayashi, K. *Protein Eng.* **1999**, *12*, 439.
(6) Carter, D. C.; Ho, J. X. *Adv. Protein Chem.* **1994**, *45*, 153.
(7) Peters. T. *All about albumin. Biochemistry, Genetics and Medical Applications*; Academic Press: San Diego, CA, 1996.
(8) He, H. M.; Carter, D. C. *Nature* **1992**, *358*, 209.
(9) Peters, T. *Adv. Protein Chem.* **1985**, *37*, 161.
(10) Curry, S.; Brick, P.; Frank, N. P. *Biochim. Biophys. Acta* **1999**, *1441*, 131.
(11) Petitpas, I.; Grune, T.; Battacharya, A. A.; Curry, S. *J. Mol. Biol.* **2001**, *314*, 955.
(12) Grelamo, E. L.; Silva, C. H. T. P.; Imasato, H.; Tabak, M. *Biochim. Biophys. Acta* **2002**, *1594*, 84.
(13) Chuang, V. T. G.; Otagiri, M. *Biochim. Biophys. Acta* **2001**, *1546*, 337.
(14) Painter, L.; Harding, M. M.; Beeby, P. J. *J. Chem. Soc., Perkin Trans.* **1998**, *18*, 3041.
(15) Lin, S. Y.; Li, M. J.; Wei, Y. S. *Spectrochim. Acta, Part A* **2004**, *60*, 3107.
(16) Krimm, S.; J. Bandekar, J. *Adv. Protein Chem.* **1986**, *38*, 181.
(17) Beauchemin, R.; N'soukpoe-Kossi, C. N.; Thomas, T. J.; Thomas, T.; Carpentier, R.; Tajmir-Riahi, H. A. *Biomacromolecules* **2007**, *8*, 3177.
(18) Byler, D. M.; Susi, H. *Biopolymers* **1986**, *25*, 469.
(19) Ahmed, A.; Tajmir-Riahi, H. A.; Carpentier, R. *FEBS Lett.* **1995**, *363*, 65.
(20) Johnson, W. C. *Proteins Struct. Funct. Genet.* **1999**, *35*, 307.
(21) Sreerama, N.; Woddy, R. W. *Anal. Biochem.* **2000**, *287*, 252.
(22) Tang, J.; Qi, S.; Chen, X. *J. Mol. Struct.* **2005**, *779*, 87.
(23) Bi, S.; Ding, L.; Tian, Y.; Song, D.; Zhou, X.; Liu, X.; Zhang, H. *J. Mol. Struct.* **2005**, *703*, 37.
(24) He, W.; Li, Y.; Xue, C.; Hu, Z.; Chen, X.; Sheng, F. *Bioorg. Med. Chem.* **2005**, *13*, 1837.
(25) Dufour, C.; Dangles, O. *Biochim. Biophys. Acta* **2005**, *1721*, 164.
(26) Ahmed Ouameur, A.; Diamantoglou, S.; Sedaghat-Herati, M. R.; Nafisi, Sh.; Carpentier, R.; Tajmir-Riahi, H. A. *Cell Biochem. Biophys.* **2006**, *45*, 203.
(27) Boulkanz, L.; Balcarand, N.; Baron, M. H. *Appl. Spectrosc.* **1995**, *49*, 1737.
(28) Bramanti, E.; Benedetti, E. *Biopolymers* **1996**, *38*, 639.

(29) Liu, J.; Tian, J.; Hu, Z.; Chen, X. *Biopolymers* **2004**, *73*, 443.

(30) Dockal, M.; Chang, C.; Carter, D. C.; Ruker, F. *Protein Sci.* **2000**, *9*, 1455.

(31) Soto, C.; Catanto, E. M. *Biochem. J.* **1996**, *314*, 701.

(32) Goormaghtigh, E.; Cabiaux, V.; Ruysschaert, J. M. *Eur. J. Biochem.* **1990**, *193*, 409.

(33) Lakowicz, J. R. *Principles of Fluorescence Spectroscopy*, 2nd ed.; Kluwer/Plenum: New York, 1999.

(34) Kragh-Hansen, U. *Dan. Med. Bull.* **1990**, *37*, 57.

(35) N'soukpoé-Kossi, C. N.; Sedaghat-Herati, M. R.; Ragi, C.; Hotchandani, S.; Tajmir-Riahi, H. A. *Int. J. Biol. Macromol.* **2007**, *40*, 484.

(36) Liang, L.; Tajmir-Riahi, H. A.; Subirade, M. *Biomacromolecules* **2008**, *9*, 50.

(37) Sulkowska, A. *J. Mol. Struct.* **2002**, *614*, 227.

(38) Ward, L. D. *Methods Enzymol.* **1985**, *117*, 400.

(39) Huang, B. X.; Dass, C.; Kim, Y.-H. *Biochem. J.* **2005**, *387*, 695.

(40) Eftink, M. R.; Ghiron, C. A. *Anal. Chem.* **1981**, *114*, 199.

(41) Jiang, C. Q.; Gao, M. X.; He, J. X. *Anal. Chim. Acta* **2002**, *452*, 185.

(42) Min, J.; Mang-Xia, X.; Dong, Z.; Yuan, L.; Xiao-Yu, L.; Xing, C. *J. Mol. Struct.* **2004**, *692*, 641.

JP8092012